

CuO nanoparticles induce cytotoxicity and apoptosis in human K562 cancer cell line via mitochondrial pathway, through reactive oxygen species and P53

Maryam Shafagh ¹, Fatemeh Rahmani ^{1*}, Norouz Delirezh ²

¹ Department of Biology and Institute of Biotechnology, Faculty of Sciences, Urmia University, Urmia, Iran

² Microbiology Department, Faculty of Veterinary Medicine, Urmia University, Urmia, Iran

ARTICLE INFO	ABSTRACT
<p>Article type: Original article</p> <hr/> <p>Article history: Received: Mar 10, 2015 Accepted: Jul 23, 2015</p> <hr/> <p>Keywords: Apoptosis Bax/Bcl-2 CuO nanoparticles K562 P53 ROS Cancer</p>	<p>Objective(s): This study focused on determining cytotoxic effects of copper oxide nanoparticles (CuO NPs) on chronic myeloid leukemia (CML) K562 cell line in a cell-specific manner and its possible mechanism of cell death. We investigated the cytotoxicity of CuO NPs against K562 cell line (cancerous cell) and peripheral blood mononuclear cell (normal cell).</p> <p>Materials and Methods: The toxicity was evaluated using cell viability, oxidative stress and apoptosis detection. In addition, the expression levels of P53, Caspase 3, Bcl-2, and Bax genes in K562 cells were studied by reverse transcription polymerase chain reaction (RT-PCR) analysis.</p> <p>Results: CuO NPs exerted distinct effects on cell viability via selective killing of cancer cells in a dose-dependent manner while not impacting normal cells in MTT assay. The dose-dependent cytotoxicity of CuO NPs against K562 cells was shown through reactive oxygen species (ROS) generation. The CuO NPs induced apoptosis was confirmed through acridine orange and propidium iodide double staining. Tumor suppressor gene P53 was up regulated due to CuO NPs exposure, and increase in Bax/Bcl-2 ratio suggested mitochondria-mediated pathway is involved in CuO NPs induced apoptosis. We also observed that Caspase 3 gene expression remained unchanged up to 24 hr exposure.</p> <p>Conclusion: These molecular alterations provide an insight into CuO NPs-caused inhibition of growth, generation of ROS, and apoptotic death of K562 cells.</p>

► Please cite this article as:

Shafagh M, Rahmani F, Delirezh N. CuO nanoparticles induce cytotoxicity and apoptosis in human K562 cancer cell line via mitochondrial pathway, through reactive oxygen species and P53. Iran J Basic Med Sci 2015; 18:993-1000.

Introduction

Chronic myelogenous leukemia (CML) is a myeloproliferative disorder (1). Many cancers such as CML initially respond to cancer therapy but later develop resistance and drawback chemotherapy (2). Therefore, it is urgent to develop new effective anticancer drugs, with more cancer cell targeting and better normal cell sparing (3). Nowadays, nanomaterials are prepared with various techniques in different shapes and diameters and are used in all human daily applications such as in medicine, solar cells, water purification, pharmaceutical, catalysis, drug delivery, cell imaging, and cancer therapy (4). Applications of CuO-NPs are also very important as antibacterial, in thermal conductivity and batteries (5). CuO nanoparticles induce generation of reactive oxygen species (ROS) oxidative stress which causes DNA damage and increases death receptor expression (6).

Apoptosis is a key mechanism in cancer development and progression. Cancer cells avoid apoptosis and continue to propagate. Apoptosis is mediated by ROS generation and oxidative stress (7). There are several genes involved in apoptotic cell

death. P53 protein triggers cell cycle arrest in the presence of DNA damage or cellular stress, to provide time for repairing of damage or self-mediated apoptosis (8). The Bcl-2 family including Bcl-2 and Bax contribute to apoptosis regulation. In particular, antiapoptotic members of the Bcl-2 family, such as Bcl-2, act to prevent or delay cell death, whereas the pro-apoptotic Bax promotes apoptosis (9). The ratio of Bax/Bcl-2 protein determines the life or death of cells in response to an apoptotic stimulus. An increase in Bax/Bcl-2 ratio decreases the cellular resistance to apoptotic stimuli, leading to apoptosis induction (10). Recently, several lines of evidence have suggested that the Caspase family plays vital roles in apoptosis induction (11).

This study aimed to investigate CuO NPs-induced toxicity in a cell specific manner as well as to determine the potential mechanism of toxicity. Cytotoxicity of CuO NPs was examined in cancer cells (human chronic myelogenous leukemia cell-line K562) and normal cells (peripheral blood mononucleated cells PBMCs). The possible mechanisms of cytotoxicity were studied using parameters such as cell viability, oxidative stress,

*Corresponding author: Department of Biology and Institute of Biotechnology, Faculty of Sciences, Urmia University, Urmia, Iran. Tel: +98-4432752117; Fax: +98-4412753172; email: frahmani@urmia.ac.ir

and apoptosis in K562 cells. Moreover, the mRNA levels of apoptotic genes P53, Bax, Caspase 3, and anti-apoptotic Bcl-2 gene were assayed by RT-PCR analysis.

Materials and Methods

Materials

Copper oxide nano powder (20 nm, purity > 99 %) was purchased from Iranian Nanomaterials Pioneers Company, NANOSANY (Mashhad, Iran). RPMI-1640 medium and fetal bovine serum (FBS) was obtained from GIBCO, GIBCO/Life Technologies Inc. (Gaithersburg, MD, USA). MTT [3-(4, 5-2-yl)-2-diphenyltetrazoliumbromide] and 2,7-dichloro-fluoresceindiacetate (DCFH-DA) and Trizol reagent were purchased from Sigma-Aldrich (St Louis, MO, USA). The first strand cDNA synthesis kit (Fermentas) and PCR primers were purchased from Sinaclone Company (Tehran, Iran).

Characterization of CuO nanoparticles

X-ray diffraction (XRD) pattern was used to determine the crystalline nature of CuO NPs. The XRD pattern of CuO NPs was acquired at room temperature with the help of PANalytical X'Pert ProTM X-ray diffractometer equipped with a Ni filter using Cu K α ($\lambda = 1.54056 \text{ \AA}$) radiations as X-ray source. Morphology of CuO NPs was examined by transmission electron microscopy (TEM).

Preparation of CuO NPs suspension

CuO nano powder was exposed to UV illumination for 30 min before use to avoid bacterial contamination. The CuO NPs were suspended in cell culture medium and diluted to appropriate concentrations (2, 5, 10, 25 $\mu\text{g/ml}$). Prior to cells exposure, the dilutions of CuO NPs were sonicated using a sonicator bath at room temperature for 10 min at 40 W. Selection of 2–25 $\mu\text{g/ml}$ dosage range of CuO NPs was based on preliminary dose–response experiments (data not shown).

Cell culture

One type of cancer cells (K562) and one type of normal cells (PBMCs) were used to determine the cell viability against CuO NPs exposure. The human myeloid leukemia K562 cells were obtained from Pasture Institute of Iran, Tehran, Iran. Fresh peripheral blood was taken with informed consent from three healthy volunteers into sterile falcon tubes containing heparin (200 IU/ml). Human peripheral blood mononuclear cells (PBMC) were isolated by using 1.077 g/ml Ficoll/Hypaque as previously described (12). The K562 cell line was cultured in a 25 cm² culture flask in RPMI-1640 supplemented with 10% FBS, 50 mg/ml streptomycin, 50 units/ml penicillin at 37 °C in a humidified atmosphere of 5% CO₂-95% air.

Cell viability assay

Viability of cancer and normal cells against CuO NPs exposure was examined by MTT assay as described by Mossman (13). In brief, 1×10^4 cells/well were seeded in 96-well plates and exposed to different concentrations of CuO NPs for 24 hr. Four hours before termination, 20 μl of MTT (5 mg/ml) was added to each well and incubated at 37 °C for 4 hr until a purple colored formazan product developed. Then, 100 μl of DMSO (dimethyl sulfoxide) was added and plate incubated at 37 °C for 10 min to dissolve the purple crystals. The optical density (OD) values of each well were measured at 492 nm by using ELISA plate reader (Dana 3200, Iran).

Measurement of ROS

Intracellular ROS was detected by using DCFH-DA staining (14). The DCFH-DA passively enters the cell where it reacts with ROS to form the highly fluorescent compound dichlorofluorescein (DCF). 1×10^6 cells/well were seeded in 6-well plates and treated with various concentrations of nano CuO for 24 hr and then washed twice with phosphate buffered saline (PBS) and stained with 20 μM DCFH-DA for 30 min. At the end of DCFH-DA incubation, cells were washed with PBS and the fluorescence intensities were measured by flow cytometry (Beckman-Coulter), with an excitation wavelength of 488 nm and an emission wavelength of 525 nm. Furthermore, the control and treated cells were visualized using a fluorescence microscope (Olympus CKX 41) by grabbing the images at 40 \times magnification.

Detection of apoptosis by acridine orange and propidium iodide

CuO NPs induced death of K562 cells was quantified using acridine orange and propidium iodide double staining (15). Briefly, treatment was carried out in a 6-well microplate. The K562 cells were plated at a concentration of 1×10^6 cells/ml and treated with CuO NPs at different concentrations (0, 2, 5, 10, 25 $\mu\text{g/ml}$). The cells were incubated in 5% CO₂ atmosphere at 37 °C for 24 hr. The supernatant was discarded and the cells were washed twice using PBS. A 10 μl of fluorescent dyes containing acridine orange (10 $\mu\text{g/ml}$) and Propidium Iodide (10 $\mu\text{g/ml}$) were added into the cellular pellet at equal volumes of each. The percentage of apoptotic cells was determined in an improved Neubauer rhodium hemocytometer under fluorescent microscopy (Olympus CKX41).

Detection of mRNA expressions using reverse transcription-PCR

The total RNA was extracted using Trizol reagent. One microgram of total RNA was reverse transcribed using Oligo (dT)₁₈ primer in a 20 μl reaction mixture with RevertAid M-MuLV reverse

Table 1. Gene-specific primers used for reverse transcription polymerase chain reaction (RT-PCR)

Gene name	Primer sequences
Caspase 3 (400bp)	Fwd- 5'-TTTGTTTGTGTGCTTCTGAGCC-3' Rev- 5'-ATTCTGTTGCCACCTTTTCGG-3'
P53 (293bp)	Fwd- 5'-CAGCCAAGTCTGTGACTTGACACGTAC-3' Rev- 5'-CTATGTCGAAAAGTGTTCGTGCATC-3'
Bax (250bp)	Fwd- 5'-TGCTTCAGGGTTTCATCCAGG-3' Rev- 5'-TGGCAAAGTAGAAAAGGGCGA-3'
Bcl-2 (478bp)	Fwd- 5'-CTACGAGTGGGATGCGGGAGATG-3' Rev- 5'-GGTTCAGGTACTCAGTCATCCACAG-3'
β - actin (243bp)	Fwd- 5'-CTTCTACAATGAGCTGCGTG-3' Rev- 5'-TCATGAGGTAGTCAGTCAGG-3'

transcriptase according to manufacturer's instructions (Fermentas). The related PCR primers listed in Table 1 were used to produce the respective correlated products. The PCRs for β -actin, P53, Bax, Caspase 3 cDNAs were performed with 30 amplification cycles as follows: denaturation at 94 °C for 1 min, annealing for 40 sec at 50 °C for Caspase 3 and β -actin, at 55 °C for Bax, at 58 °C for P53, followed by extension at 72 °C for 45 sec. The PCRs for Bcl-2 cDNA was performed with 35 amplification cycles and the reaction condition was: denaturation at 94 °C for 1 min, annealing at 58 °C for 40 sec and extension at 72 °C for 45 sec. The PCR products were analyzed on 1.5% agarose gel containing ethidium bromide. For densitometric analysis, band intensity was assessed using gel documentation (Gel Logic Pro 212 Imaging System, USA). After band intensity was adjusted by β -actin intensity, data were calculated as the mean \pm standard deviation of at least three experiments.

Statistical analysis

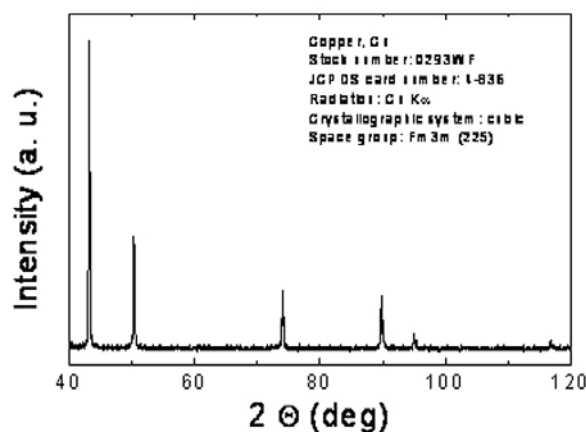
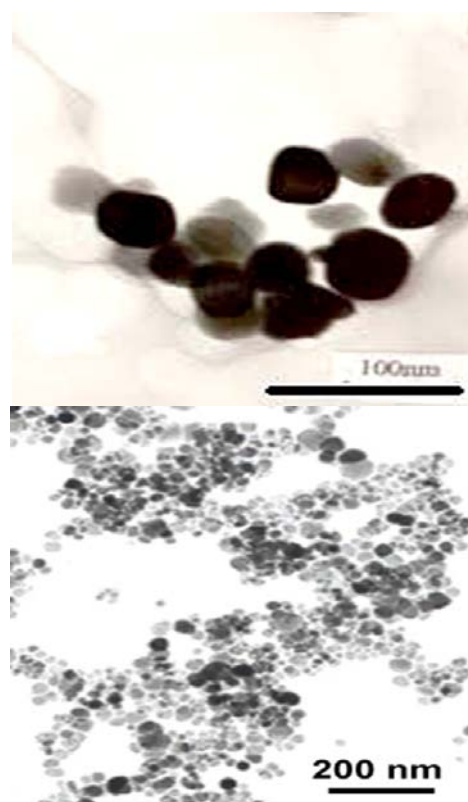
The data were analyzed by one-way analysis of variance (ANOVA) and statistical significance was determined by means of Statistical Package for Social Science (version 20; SPSS Inc, Chicago, IL) followed by Dunnett's multiple comparison tests and are presented as means \pm SDs. *P*-values of less than 0.05 were considered statistically significant.

Results

Physicochemical characterization of CuO nanoparticle

Figure 1 shows X-ray diffraction patterns of CuO NPs that clearly exhibits the crystalline nature of these particles. The average crystal size is 20 nm which is calculated using Debye-Scherrer formula. $D = 0.89 \lambda / \beta \cos \theta$ where λ is the X-ray wavelength (1.5406), β is the peak width, and theta is the Bragg's angle. The presence of sharp structural peaks in XRD patterns and average crystallite size less than 25 nm suggested the nano nature of the particles.

Figure 2 shows the typical TEM image of CuO NPs with exhibition of majority of the particles in spherical shape and smooth surfaces. The average TEM diameter of CuO NPs was 20 nm, supporting the XRD data.

**Figure 1.** X-ray diffractogram for the copper oxide nanoparticles**Figure 2.** Transmission electron microscopy (TEM) image of copper oxide nanoparticles

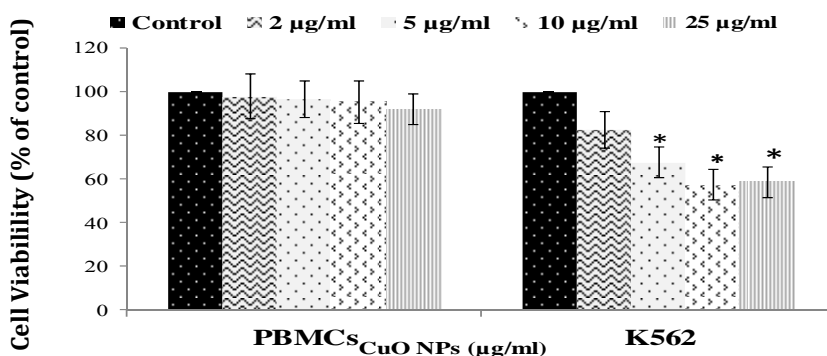


Figure 3. The effect of CuO NPs on the viability of K562 cells and peripheral blood mononucleated cells (PBMCs). Data represented as mean±SD of three identical experiments made in three replicates. **P*<0.05 statistically significant differences as compared with the control group

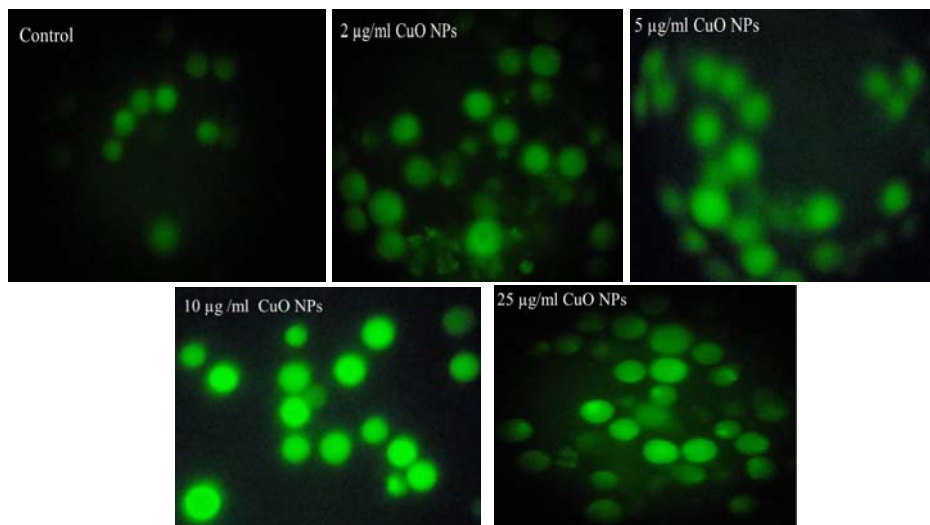
Selective cytotoxicity of CuO nanoparticles against cancer cells

MTT results showed that CuO NPs significantly decreased the viability of K562 in a dose-dependent manner. At 10 µg/ml, cell viability was significantly decreased to 57% for the K562 cells (*P*<0.05). However, CuO NPs did not induce significant reduction in the viability of normal cells (PBMCs) up to the optimum concentration of 10 µg/ml, used in this study (Figure 3).

CuO NPs induced ROS generation in K562 cell line

ROS generation was detected following exposure to CuO NPs by the fluorophore H2DCF-DA in K562 cell line. The cells exposed to 10 and 25 µg/ml CuO for 24 hr showed a significant increase in the ROS generation and fluorescent microscopy data revealed induction of intracellular production of ROS in a dose-dependent manner (Figure 4). The number of DCF-positive cells was increased after exposure to nano-CuO (*P*<0.05).

A)



B)

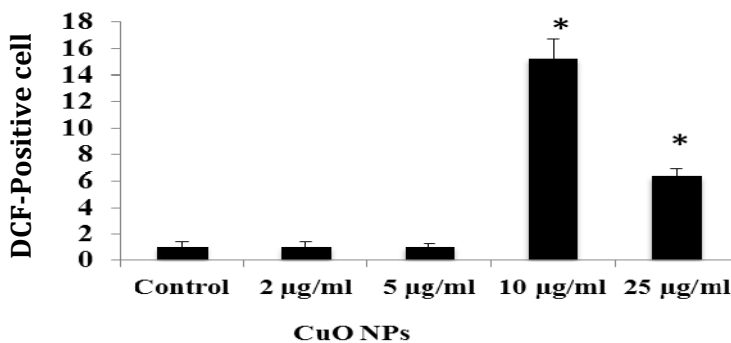


Figure 4. CuO NPs induced dose-dependent oxidative stress in K562 cell. A) A reactive oxygen species production detected by DCF-DA staining in K562 cells treated with 0, 2, 5, 10 and 25 µg/ml CuO NPs for 24 hr. B) The gated percentage of K562 cells for DCF-DA staining. Data represented as mean ± SD. Asterisk, statistically significant difference compared with control (*P*<0.05)

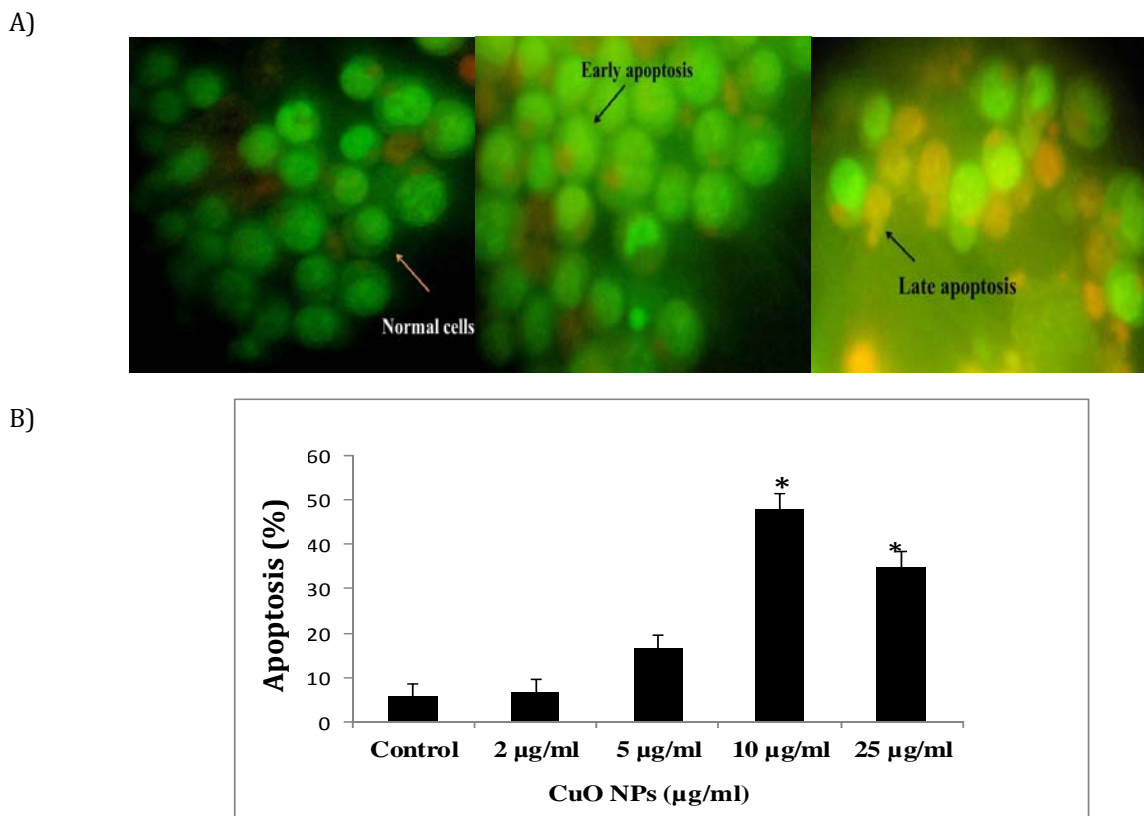


Figure 5. Evaluation of apoptosis in K562 cancer cells after co-culture with different concentrations of CuO NPs for 24 hr. A) K562 apoptosis was assessed by acridine orange/propidium staining. The green cells with diffused chromatin are viable, and red cells with condensed chromatin are apoptotic, early apoptosis features were seen after 24 hr, representing intercalated acridine orange (bright green) amongst the fragmented DNA (arrow). B) K562 cell death via apoptosis increased significantly (* $P < 0.05$) in a dose-dependent manner

Quantification of apoptosis using acridine orange and propidium iodide double staining

In cell populations, the green cells (excluding propidium iodide) with diffused chromatin are viable, green cells with condensed chromatin are apoptotic and red cells (including propidium iodide) with non-condensed chromatin are necrotic. A total of 100 cells were used arbitrarily and differentially, together with untreated negative control cells for scoring. Results show that CuO NPs triggered morphological changes in treated K562 cells indicating possible induction of apoptosis upon treatment in a dose-dependent manner (Figure 5).

Effects of CuO NPs on apoptosis-associated genes

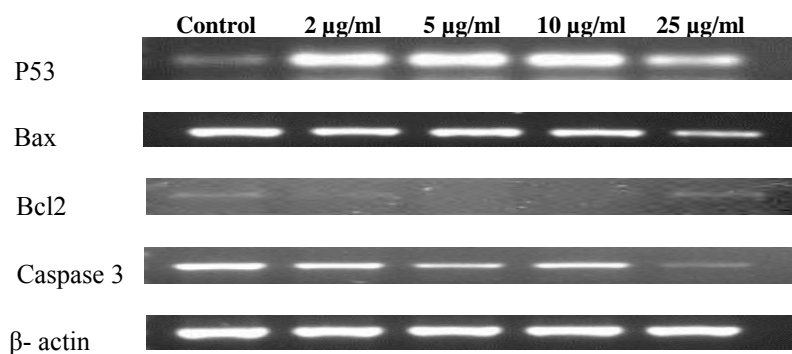
When K562 cells were treated with CuO NPs for 24 hr, the level of P53 mRNA in K562 cells was significantly up regulated (Figure 6). Exposure of K562 cells to CuO NPs resulted in down regulating the expression of Bcl-2, while it did not alter the expression level of Bax (Figure 6). However, relative ratio of Bax/Bcl-2 in CuO NPs treated K562 cells increased significantly ($P < 0.05$). Moreover, CuO NPs had no effect on the transcript level of Caspase 3 (Figure 6).

Discussion

One of the major challenges in cancer therapy is to improving therapeutic effectiveness of anticancer drugs and reducing their adverse effects to improve quality of life for cancer patients (16). In our MTT cytotoxicity screening assay, CuO NPs showed a broad spectrum of cytotoxicity with most activity on K562 cells but not on normal PBMCs cells. One of the main challenges facing cancer chemotherapy is the inability of anticancer drugs to effectively distinguish cancer cells. Although, cancer-specific toxicity of CuO is still not clear, but selectivity in the killing of cancer cells by CuO NPs is clinically important.

Recently, selective cytotoxicity of other nanoparticles including zinc oxide (ZnO) and iron oxide (Fe_3O_4) nanoparticles on cancer cells has been reported. Premanathan *et al* (2011) observed that ZnO nanoparticles exhibited a preferential ability to kill human myeloblastic leukemia cells (HL60) as compared to normal peripheral blood mononuclear cells (PBMCs) (17). In 2013, Ahamed *et al* observed that Fe_3O_4 NPs have selective effects on cell viability and killing of cancer cells (HepG2 and A549) while posing no effect on normal (rat hepatocytes and IMR-90) cells (18).

A)



B)

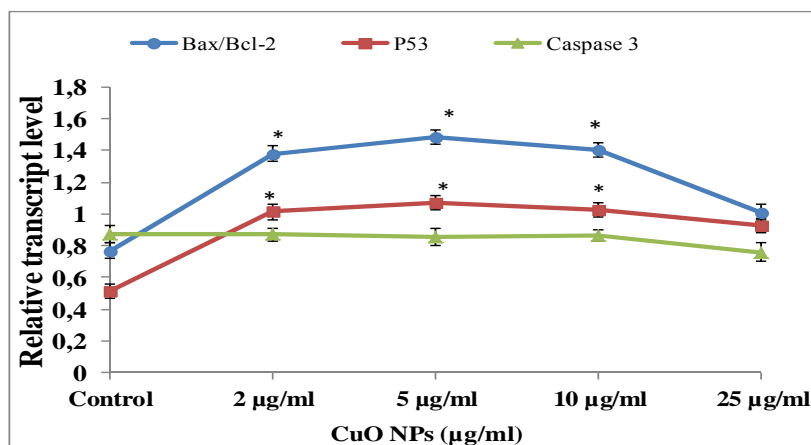


Figure 6. Determination of changes in transcript profiling of P53, Bax, Bcl-2 and Caspase 3 by semi quantitative RT-PCR. A) RT-PCR analysis of CuO NPs treated K562 cells. The mRNA was isolated from K562 cells treated with CuO NPs by 0, 2, 5, 10, and 25 μ g/ml for 24 hr. Each blot is representative of three similar experiments. B) Analysis of the fluorescent intensity of each band. The expression of P53, Bax, Bcl-2 and Caspase 3 mRNA was normalized to β -actin level. The data are expressed as mean \pm standard deviation (SD) (n= 3). * $P < 0.05$ statistically significant differences as compared with the control group

Current developments in cancer research suggest that generation of ROS through oxidative stress is a common mechanistic pathway of a number of apoptotic stimuli (19). ROS has been an essential signaling molecule for the initiation and execution of apoptosis (7). Toxicity of CuO NPs in different human cell lines e.g. human lung epithelial (A549) (20), human cardiac microvascular endothelial (HCMEC) (21), and human hepato carcinoma cell line (HepG2) (22) has been indicated through oxidative stress. In another study, N2A cells were found to be less sensitive to CuO NPs effects than the others (23). Interestingly, the cytotoxicity of CuO NPs toward mammalian cells depends on the cell type.

In our study, CuO NPs induced ROS generation in K562 cancer cells and apoptosis was observed in K562 cells exposed to 10 and 25 μ g/ml of nano-CuO. Our MTT cytotoxic results of CuO NPs on K562 cells confirmed morphological changes. Morphologic description using fluorescence microscopy is one of the best ways to define apoptosis (24). In the present study, copper oxide NPs treatment caused increase

in the percentage of the cells in early and late phases of apoptosis. The mechanistic pathways of nanoparticles to induce cellular damage and cell death induction are not yet fully understood. However, studies suggest that P53 plays a central role in the cellular response to ROS-induced DNA damage and apoptosis (25). In general, P53 exists in an inactive state at low concentrations in cells, activated only when cells have undergone stress, resulting in the accumulation of P53 (26) and blockage of the progression of the cell cycle. This phenomenon triggers cell-cycle arrest to provide time for DNA repair or for self-mediated apoptosis (8). Moreover, this protein down regulates anti-apoptotic Bcl-2 proteins and trans-activates Puma, Noxa and pro-apoptotic Bax to trigger the mitochondrial pathway of apoptosis (27).

Members of the Bcl-2 family of proteins are associated with the mitochondrial membrane and regulate its integrity (28). Hence, an alteration in relative ratios of Bax/Bcl2 could determine how

much cellular stress is needed to induce apoptosis (10). We detected alteration in expression of genes involved in the damage response pathway using RT-PCR analysis. Our results indicate that CuO NPs increase P53 mRNA level while decreasing the level of anti-apoptotic Bcl-2 transcript. Since, CuO NPs treatment had no effect on the Bax mRNA level; thereby the Bax/Bcl-2 ratio has been increased. Based on the Zhang *et al* (1999) study, tamoxifen-induced apoptosis in breast cancer cells is related to down regulation of Bcl-2, with no alteration of P53 protein level (29). This is consistent with previous study that reported ionizing radiation induces down regulation of Bcl-2 mRNA expression (30). This suggests that alteration of Bcl-2 protein alone is sufficient to change the Bax/Bcl-2 ratio. Alteration of Bcl-2 protein could also decrease the antiapoptotic levels which consequently alters susceptibility to apoptosis. The results are in line with an earlier study conducted by Mroz *et al* (2008) which documented that nanoparticles and ROS may induce DNA damage and activate P53 (31). Increase in Bax/Bcl-2 ratio followed by activation of P53 accelerates the release of the apoptosis-inducing factor and cytochrome c from mitochondria, thus activating the Caspase cascade (32). Activated Caspase 3 is capable of autocatalytic activation of other Caspases, leading to rapid and irreversible apoptosis (33). Unexpectedly, in this research, CuO NPs had no effect on the Caspase 3 transcript level. This finding is supported by another study demonstrating that cardiotoxin III had no appreciable effect on Caspase 3 transcript level in K562 cells while regulating this gene at the protein level (34). Our data also suggest that nano-CuO activated P53-mediated apoptosis response is in a dose-dependent manner. Further research should be conducted to investigate Caspase 3 at protein level. In all experiments, the cytotoxicity and apoptotic effect of CuO NPs was reduced at 25 µg/ml compared to 10 µg/ml. This reduction may be due to agglomeration of NPs in higher concentrations, which diminishes its effect.

Conclusion

CuO NPs showed selective cytotoxicity towards K562 cell line. This compound is potentially a good anti-cancer drug since it does not kill healthy cells. The present work also suggests CuO NPs induction of apoptosis is mediated through the ROS production in cancer cells. In our study, all experiments provided a clear picture of the molecular ordering of CuO-induced apoptosis, starting with the P53 up regulation. Therefore, modulation of P53 and Bax/Bcl-2 may be a key mechanism underlying apoptosis of K562 cells. Further research must be carried out on other cancer and normal cells to determine whether anticancer effect of CuO NPs is a

universal mechanism. Present study also warrants further investigation such as assessment of Caspase 3 activity.

Acknowledgment

This study was partially sponsored by Urmia University, Urmia, Iran. The results reported in this paper were part of a student thesis.

References

1. Deininger MW, Goldman JM, Melo JV. The molecular biology of chronic myeloid leukemia. *Blood* 2000; 96:3343-3356.
2. Druker BJ, Guilhot F, O'Brien SG, Gathmann I, Kantarjian H, Gattermann N, *et al*. Five year follow-up of patients receiving imatinib for chronic myeloid leukemia. *N Engl J Med* 2006; 355:2408-2417.
3. Rasmussen JW, Martinez E, Louka P, Wingett DG. Zinc oxide nanoparticles for selective destruction of tumor cells and potential for drug delivery applications. *Expert Opin Drug Deliv* 2012; 7:1063-1077.
4. Manimaran R, Palaniradja K, Alagumurthi N, Sendhilnathan S, Hussain J. Preparation and characterization of copper oxide nanofluid for heat transfer applications. *Appl Nanosci* 2014; 4:163-167.
5. Chang YN, Zhang M, Xia L, Zhang J, Xing L. The toxic effects and mechanisms of CuO and ZnO nanoparticles. *Materials* 2012; 5:2850-2871.
6. Yang H, Liu C, Yang DF, Zhang HS, Xi Z. Comparative study of cytotoxicity, oxidative stress and genotoxicity induced by four typical nanomaterials: The role of particle size, shape and composition. *J Appl Toxicol* 2009; 29:69-78.
7. Ott M, Gogvadze V, Orrenius S, Zhivotovsky B. Mitochondria, oxidative stress and cell death. *Apoptosis* 2007; 12:913-922.
8. Li T, Kon N, Jiang L, Tan M, Ludwig T, Zhao Y, *et al*. Tumor suppression in the absence of P53-mediated cell-cycle arrest, apoptosis, and senescence. *Cell* 2012; 149:1269-1283.
9. Antonsson B, Martinou JC. The Bcl-2 protein family. *Exp Cell Res* 2000; 256:50-57.
10. Chougule M, Patel AR, Sachdeva P, Jackson T, Singh M. Anticancer activity of Noscapine, an opioid alkaloid in combination with cisplatin in human non-small cell lung cancer. *Lung Cancer* 2011; 71:271-282.
11. Green DR, Reed JC. Mitochondria and apoptosis. *Science* 1998; 281:1309-1312.
12. Boyum A. Separation of leukocytes from blood and bone marrow. Introduction. *Scand J Clin Lab Invest Suppl* 1968; 97:7-11.
13. Mossman T. Rapid colorimetric assay for cellular growth and survival: application to proliferation and cytotoxicity assays. *J Immunol Methods* 1983; 65:55-63.
14. Elbekai RH, El-Kadi AOS. The role of oxidative stress in the modulation of aryl hydrocarbon receptor-regulated genes by As3+, Cd2+ and Cr6+. *Free Radic Biol Med* 2005; 39:1499-1511.
15. Ali R, Alabs AM, Ali AM, Ideris A, Omar AR, Yusoff K, *et al*. Cytolytic effects and apoptosis induction of new castle disease virus strain AF2240 on anaplastic astrocytoma brain tumor cell line. *Neurochem Res* 2011; 36:2051-2062.

16. Wu YN, Yang LX, Shi XY, Li IC, Biazik JM, Ratinac KR, *et al.* The selective growth inhibition of oral cancer by iron core-gold shell nanoparticles through mitochondria-mediated autophagy. *Biomaterials* 2011; 32:4565–4573.
17. Premanathan M, Karthikeyan K, Jayasubramanian K, Manivannan G. Selective toxicity of ZnO nanoparticles toward Gram positive bacteria and cancer cells by apoptosis through lipid peroxidation. *Nanomedicine* 2011; 7:184–192.
18. Ahamed M, Alhadlaq HA, Khan MAM, Akhtar MJ. Selective killing of cancer cells by iron oxide nanoparticles mediated through reactive oxygen species via P53 pathway. *J Nanopart Res* 2013; 15:1225.
19. Ryter SW, Kim HP, Hoetzel A, Park JW, Nakahira K, Wang X, *et al.* Mechanisms of cell death in oxidative stress. *Antioxid Redox Signal* 2007; 9:49–89.
20. Ahamed M, Siddiqui MA, Akhtar MJ, Ahmad I, Pant AB, Alhadlaq HA. Genotoxic potential of copper oxide nanoparticles in human lung epithelial cells. *Biochem Biophys Res Commun* 2010; 396:578–583.
21. Sun J, Wang S, Zhao D, Hun FH, Weng L, Liu H. Cytotoxicity, permeability, and inflammation of metal oxide nanoparticles in human cardiac micro-vascular endothelial cells: cytotoxicity, permeability, and inflammation of metal oxide nanoparticles. *Cell Biol Toxicol* 2011; 27:333–342.
22. Siddiqui MA, Alhadlaq HA, Ahmad J, Al-Khedhairi AA, Musarrat J, Ahamed M. Copper oxide nanoparticles induced mitochondria mediated apoptosis in human hepato carcinoma cells. *PLoS One* 2013; 8:e69534.
23. Perreault F, Melegari SP, Costa CH, Siddi-Rossetto AF, Popovic R, Matias WG. Genotoxic effects of copper oxide nanoparticles in Neuro2A cell cultures. *Sci Total Environ* 2012; 441: 117–124.
24. Doonan F, Cotter TG. Morphological assessment of apoptosis. *Methods* 2008; 44:200–204.
25. Chowdhury R, Chowdhury S, Roychoudhury P, Mandal C, Chaudhuri K. Arsenic induced apoptosis in malignant melanoma cells is enhanced by menadione through ROS generation, p38 signaling and P53 activation. *Apoptosis* 2009; 14:108–123.
26. Hussain SM, Hess KL, Gearhart JM, Geiss KT, Schlager JJ. *In vitro* toxicity of nanoparticles in BRL 3A rat liver cells. *Toxicol in vitro* 2005; 19:975–983.
27. Miyashita T, Krajewski S, Krajewska M, Wang HG, Lin HK, Liebermann DA, *et al.* Tumor suppressor P53 is regulator of bcl-2 and bax gene expression *in vitro* and *in vivo*. *Oncogene* 1994; 9:1799.
28. Adams JM, Cory S. The Bcl-2 protein family: arbiters of cell survival. *Science* 1998; 281:1322–1326.
29. Zhang GJ, Kimijima I, Onda M, Kanno M, Sato H, Watanabe T, *et al.* Tamoxifen-induced apoptosis in breast cancer cells relates to down regulation of Bcl-2, but not Bax and Bcl-xL, without alteration of P53 protein levels. *Clin Cancer Res* 1999; 5:2971–2977.
30. Chen M, Quintans J, Fuks Z, Thompson C, Kufe DW, Weichselbaum RR. Suppression of Bcl-2 messenger RNA production may mediate apoptosis after ionizing radiation, tumor necrosis factor α , and ceramide. *Cancer Res* 1995; 55:991–994.
31. Mroz RM, Schins RP, Li H, Jimenez LA, Drost EM, Holownia A, *et al.* Nanoparticle driven DNA damage mimics irradiation-related carcinogenesis pathways. *Eur Respir J* 2008; 31:241–251.
32. Yang SH, Lu MC, Chien CM, Tsai CH, Lu YJ, Hour TC, *et al.* Induction of apoptosis in human leukemia K562 cells by cardiotoxin III. *Life Sci* 2005; 76:2513–2522.
33. Sánchez-Pérez Y, Chirino YI, Osornio-Vargas AR, Morales-Bárceñas R, Gutiérrez-Ruiz C, Vázquez-López L, *et al.* DNA damage response of A549 cells treated with particulate matter (PM10) of urban air pollutants. *Cancer Lett* 2009; 278:192–200.
34. Yang SH, Tsai CH, Lu MC, Yang YN, Chien CM, Lin SF, *et al.* Effects of cardiotoxin III on expression of genes and proteins related to G2/M arrest and apoptosis in K562 cells. *Mol Cell Biochem* 2007; 300:185–190.